Available online at www.sciencedirect.com
SCIENCE DIRECT®
Scripta Materialia 50 (2004) 1423–1427
Scripta MATERIALIA
www.actamat-journals.com

Effect of amorphous–crystalline interfaces on the martensitic transformation in $Ti_{50}Ni_{25}Cu_{25}$

R. Santamarta [a,b], D. Schryvers [a,*]

[a] *EMAT, University of Antwerp, Groenenborgerlaan 171, B-2020 Antwerpen, Belgium*
[b] *Departament de Física, Universitat de les Illes Balears, Cra. de Valldemossa km 7.5, E-07122 Palma de Mallorca, Spain*

Received 26 February 2004; received in revised form 26 February 2004; accepted 13 March 2004

Abstract

A partially crystallized amorphous $Ti_{50}Ni_{25}Cu_{25}$ melt-spun ribbon showing spherical particles in martensite has been investigated. Microstructural observations support the hindering of the martensitic transformation as well as the production of additional autoaccommodated structures nearby the interface compared with the ones used inwards.

Keywords: Shape memory alloys (SMA); Transmission electron microscopy (TEM); Martensitic phase transformation; Amorphous–crystalline interface; Melt-spinning

1. Introduction

Almost-ready-to-use metallic ribbons may be produced by melt-spinning, avoiding complex thermomechanical treatments needed after conventional casting, and thus leading to cheaper shape memory alloys (SMA) for certain applications. However, this rapid solidification technique also introduces particular microstructures, e.g. a reduction of the grain size when increasing the wheel velocity (i.e. cooling rate) [1,2]. In certain alloys, a high cooling rate can even produce amorphous as cast melt-spun ribbons, which has been used in other fields for casting amorphous metals [3,4]. Among Ni–Ti based SMA, $Ti_{50}Ni_{50-x}Cu_x$ and $Ni_{50}Ti_{50-x}Me_x$ alloys (with Me = Hf, Zr, Nb) have been reported to be (partially) amorphous after melt-spinning when using a significant amount of the third element as well as a high cooling rate [5,6].

Although production of amorphous material may seem useless in the field of SMA, the exceptional ductility of metallic amorphous alloys can be used for shaping the materials, which will exhibit shape memory properties after crystallization. Then, modifying the crystallization parameters during the subsequent crystallization process, it might be possible to control the final crystalline structure and, therefore, some properties of the martensitic transformation. Several works on this new attractive idea have been carried out in $Ti_{50}Ni_{25}Cu_{25}$ [7,8] and $Ni_{50}Ti_{32}Hf_{18}$ [9].

In addition to that, further investigations have also been performed on completely crystallized $Ti_{50}Ni_{25}Cu_{25}$ ribbons [10–14], especially stimulated by the specific properties of these alloys. Cu substituting Ni in the binary Ni–Ti decreases the transformation hysteresis and the effect of cycling processes on the transformation, as well as the sensitivity of the transformation temperatures to composition changes [15,16]. Besides these features, the transformation sequence in Ti–Ni–Cu alloys depends on the Cu content [15]. For Cu contents below 10 at.% the monoclinic B19′ martensite is formed on cooling from the cubic B2 austenite, as in the binary Ni–Ti. The intermediate orthorhombic B19 martensite appears when the Cu concentration is approximately between 10 and 15 at.%, the transformation sequence becoming $B2 \rightarrow B19 \rightarrow B19'$. Finally, higher Cu additions shift the second step to lower temperatures and usually only the $B2 \rightarrow B19$ transformation is observed above room temperature (RT) in bulk alloys.

On the other hand, some microstructural characterization has also been performed during the first steps of the crystallization of an initially amorphous $Ti_{50}Ni_{25}Cu_{25}$ melt-spun ribbon, in which some single- and multi-grain spherical particles in austenite have

* Corresponding author. Tel.: +32-3-265-247; fax: +32-3-265-257.
E-mail addresses: ruben.santamarta@uib.es (R. Santamarta), nick.schryvers@ua.ac.be (D. Schryvers).

1359-6462/$ - see front matter
doi:10.1016/j.scriptamat.2004.03.013

been observed by transmission electron microscopy (TEM) [17,18]. The aim of the present work is to focus on similar spherical particles in martensite and in particular on the effect of the interface with the amorphous regions on the martensitic transformation.

2. Experimental procedures

An initially amorphous ribbon was prepared by single-roller melt-spinning from a pre-synthesized $Ti_{50}Ni_{25}Cu_{25}$ alloy. The bulk alloy was prepared from high purity metals by melting several times in an argon arc furnace. Afterwards, the obtained ingots were re-melted in quartz crucibles under a purified helium atmosphere and ejected onto a rotating wheel with a surface speed of 37 m/s. The cooling rate obtained during the fast solidification was around 5×10^5 K/s, producing an amorphous ribbon ~40 μm thick and 1.7 mm wide.

Pieces shorter than 3 mm were cut from this ribbon and then enclosed into quartz crucibles under high vacuum conditions. Isothermal treatments at relatively low temperatures (30 min at 420 °C or 10 min at 424 °C) have been performed in a tubular furnace followed by water quench in order to obtain partially crystalline specimens. The parameters of the thermal treatment have been selected slightly higher than the crystallization temperature, after DSC experiments carried out on the same ribbon [8], seeking for a higher control of the crystallization process.

Samples for TEM were obtained from these pieces by double jet electropolishing at ~25 V (~0.15 A) using an acetic acid solution with 8% of perchloric acid yielding plan-view samples. Conventional TEM studies have been carried out on a Philips CM-20 twin microscope operating at 200 kV and equipped with an energy dispersive X-ray (EDX) spectrometer.

3. Results

Thermal treatments around the crystallization temperature (30 min at 420 °C and 10 min at 424 °C in the present work) result in a distribution of few spherical particles around 3–5 μm or 7–8 μm, respectively, embedded in large regions of amorphous matrix. The growth of the particles and the formation of possible crystalline–crystalline grain boundaries, either by developing multi-grain particles or by contacting adjacent ones, occur at high temperatures at which the crystalline structure is austenite. On the other hand, the main structure of the particles at RT is martensite indicating a martensitic transformation upon quenching, in contrast to the smaller spherical particles that remain in austenite after a treatment of 10 min at 420 °C [17,18].

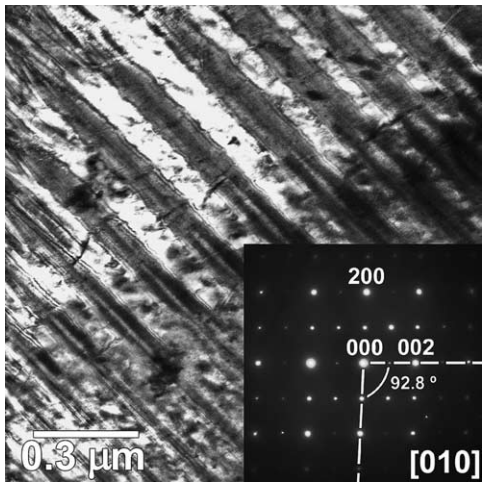

Fig. 1. Micrograph and ED (inset) of a region showing monoclinic martensite. The ED shows mainly the contribution from the variant with darker contrast in the micrograph.

Electron diffraction (ED) patterns from the particles in martensite normally show the common B19 orthorhombic martensitic phase of the $Ti_{50}Ni_{50-x}Cu_x$ system with $x \geqslant 10$ at.% Cu. This martensite is often arranged in the typical $\{1\,1\,1\}_{B19}$ type I twinning described in [19], two unique variants being sometimes extended through entire grains or particles with rather regular spacing. However, some particles showing the monoclinic phase have also been occasionally observed (Fig. 1).

Fig. 2a shows part of a spherical particle with orthorhombic martensite exhibiting a fine twinning extended almost all over the entire grain. However, a closer look to the bottom of Fig. 2a shows that the autoaccommodated martensite not always reaches the interface with the amorphous regions (Fig. 2b). This effect has often been observed at the interfaces with the amorphous regions but not at the interfaces between two different crystalline regions or particles (e.g. upper right corner of Fig. 2a). ED patterns from both regions in Fig. 2b confirm the orthorhombic martensitic structure (Fig. 2c) of the left part in Fig. 2b (i.e. inner part of the grain) and the austenitic structure (Fig. 2d) of the non-twinned region close to the interface. Moreover, the orientation relationship between both phases can be described by the lattice correspondence between B2 and B19 structures detailed in [19], indicating that the entire region belongs to the same original parent crystal.

Fig. 3a shows a section from another particle again containing twinned orthorhombic martensite. As in the previous case, the martensitic transformation is not completed nearby the interface with the amorphous region, forming a "saw-like" morphology in this zone. In order to better appreciate this special morphology, a scheme of Fig. 3a (Fig. 3b) has been drawn with the help of dark field (DF) images (Fig. 3c and d). These DF images have been obtained by selecting spots from single

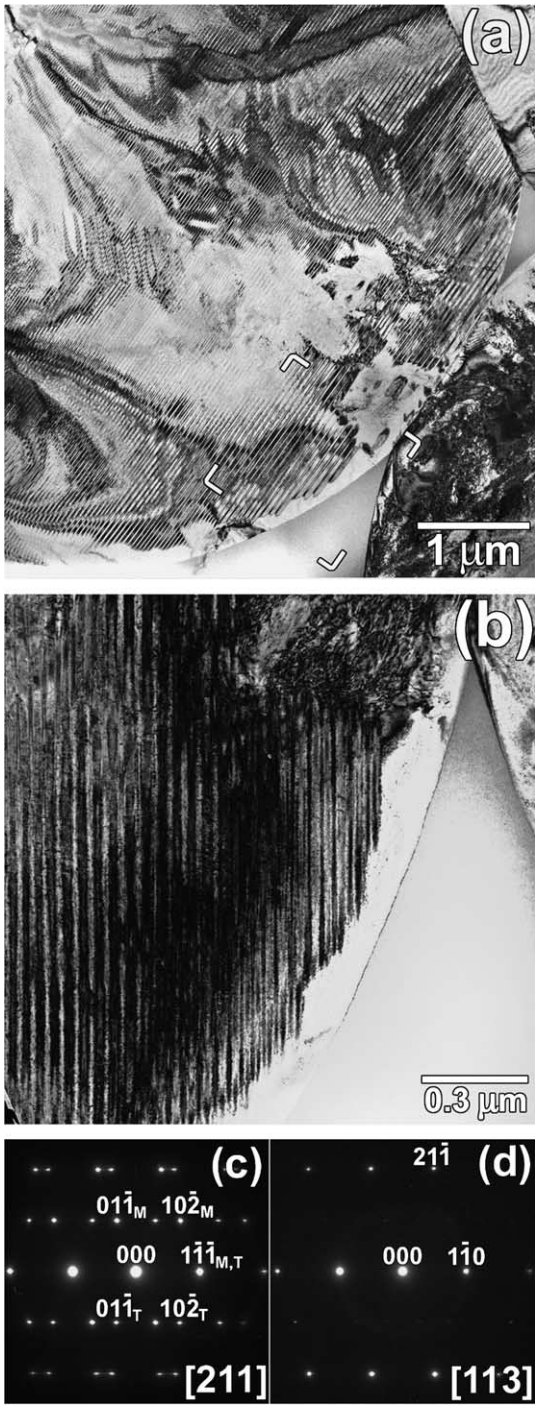

Fig. 2. (a) Micrograph of a particle with {1 1 1} type I twinning extended over the grain. (b) Micrograph in another orientation of the outlined region in (a), in which it is observed that the autoaccommodated martensite does not reach the interface with the amorphous phase. (c) and (d) ED from the inner and outer part of the crystalline region in (b).

variants, which are arbitrarily labelled as *M* and *T* (Fig. 3c and d, respectively), in the corresponding ED of the region (Fig. 3e). Variant *M* (lighter contrast in Fig. 3c) exhibits platelets that do not reach the interface; on the other hand, variant *T* (lighter contrast in Fig. 3d) grows closer to the interface, even with some tips of the platelets reaching the end of the crystalline region. The interfaces between the two martensitic variants are observed in edge-on conditions at this particular orientation and have been identified as the $(\bar{1}\,1\,1)_{B19}$ twinning planes of the autoaccommodated martensite. Half of these twin planes become austenite–martensite interfaces in the part closest to the edge where the *T* variant continues and the *M* variant has ended. The remaining twin planes end in a re-entrant corner leaving two mirrored interfaces of which the traces match with the $\{3\,3\,4\}_{B2}$ planes, which were reported to be near the B2–B19 interface in a $Ti_{40.5}Ni_{39.5}Cu_{10}$ alloy [20].

Besides the particles showing an incomplete martensitic transformation close to the interface with the amorphous regions, other particles undergoing a complete transformation at RT have also been observed (Fig. 4). In these cases, no noticeable contributions from austenite have been detected in ED from regions nearby the edge of the particles. Fig. 4a shows one completely transformed particle with orthorhombic martensite arranged in $\{1\,1\,1\}_{B19}$ type I twins in the inner region, although the twinning plane is not observed in edge-on conditions, as in the two previous cases. Instead of regions with austenite, some additional ways of autoaccommodation have been observed nearby the interface with the amorphous regions, which seem not to be required in the inner part of the particles. These supplementary defects are apparently originated as a consequence of the amorphous–crystalline interface and may be observed either only in the vicinity of the interface, as in Fig. 4a, or somewhat extended towards the central part of the particles, as shown in another particle (Fig. 4b). Although the new autoaccommodated structures likely seem to be twins, their small volume fraction and the superposition in ED patterns with contributions of the inner structure do not allow to completely determine whether their structure is purely orthorhombic, as the one in the internal part of the particle, or slightly monoclinic.

4. Discussion

The present results clearly show that the normal course of the martensitic transformation may be inhibited by the existence of a crystalline–amorphous interface (i.e. a decrease of the transformation temperatures is promoted). The surface energy of the interface likely yields the stabilization of the austenitic phase, either by lowering the Gibbs energy of the austenite or by rising the non-chemical terms in the energy balance equation of the martensitic transformation, which oppose the transformation. Indeed, the effect of the amorphous–crystalline interface on the transformation temperatures observed here seems to be the same as that of a smaller grain size reported in other works (i.e. smaller particles

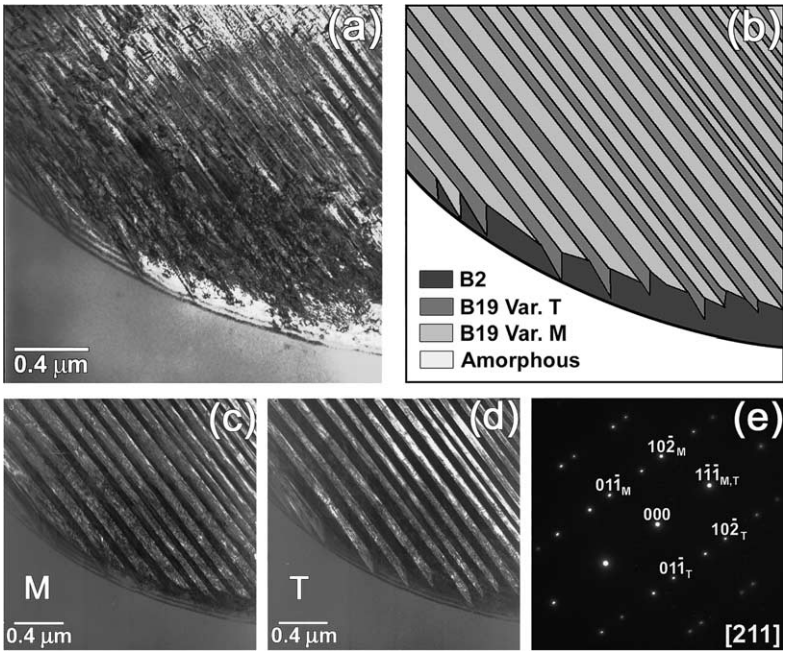

Fig. 3. (a) and (b) Micrograph and scheme, respectively, of another particle showing an incomplete martensitic transformation nearby the interface. (c) and (d) DF of the variants M and T obtained selecting the $1\,0\,\bar{2}_{M}$ and $0\,\bar{1}\,1_{T}$ spots from the ED. (e) ED from the zone in martensite.

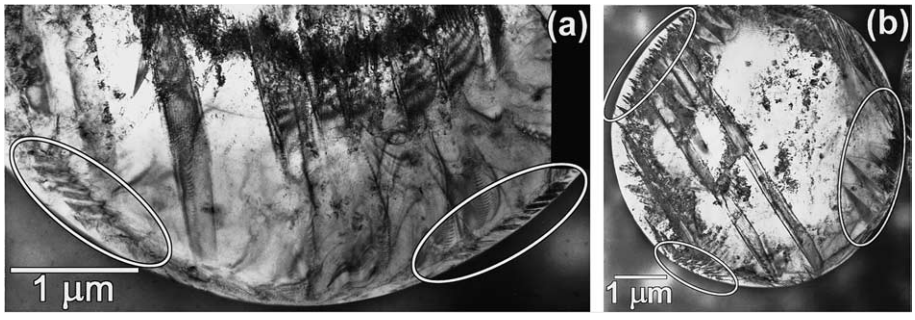

Fig. 4. (a) and (b) Two different particles showing additional autoaccommodated structures (outlined by ellipses) nearby the interface with respect to the ones used in the centre of the particles.

show lower transformation temperatures). In the case of the present crystalline particles surrounded by amorphous regions this effect becomes evident as small particles remain in austenite whereas larger ones, with the same chemical composition, are mainly in martensite [17]. The lowering of the transformation temperatures when decreasing the grain size was also traditionally attributed to the increase of the surface/volume ratio, which increases the non-chemical energy terms when grain size reduces.

However, no retained austenite has been observed at the crystalline–crystalline interfaces in the present work, either between grains in the same particle or between different particles. Therefore, it is evident that the crystalline–amorphous interface is much more effective in lowering the transformation temperatures than the crystalline–crystalline interface, probably due to a higher energy surface and, thus, a higher relaxation length. The existence of a higher energy surface in the crystalline–amorphous interface was also supposed to play an important role during the formation and growth of the multi-grain spherical particles described in [18]. This stronger decrease of the transformation temperatures would clarify the existence of smaller grains (below 1 μm) showing martensitic structures in completely crystallized $Ti_{50}Ni_{25}Cu_{25}$ samples, as pointed out in [17], whereas particles with comparable sizes are always in austenite when being surrounded by amorphous regions [17,18]. The further decrease of the transformation temperatures for crystalline particles surrounded by amorphous regions with respect to grains with similar size but surrounded by other crystalline grains was also observed for partially and completely crystallized Ni_{50}-$Ti_{32}Hf_{18}$ ribbons [9].

In addition, the results shown here demonstrate the existence of extra accommodated morphologies nearby

the amorphous interfaces of some particles, again indicating the difficulties to follow the normal transformation or accommodation near the crystalline–amorphous interface. These difficulties for the planes of the martensitic regions to adapt with the amorphous interface could be lower for some specific planes or orientations, then promoting extra single or twinned martensitic platelets in more favourable orientations. Alternatively, one variant of a previously twinned region could be further hindered with respect to the second one for the same reason, resulting in morphologies similar to the ones in Fig. 3.

Finally, the existence of a monoclinic martensite in the present $Ti_{50}Ni_{25}Cu_{25}$ alloy should be noted. The origin of this structure is not related with any deviation from the nominal composition, as the crystalline regions show the same chemical content as the amorphous matrix [17]. Thus, to some extend, the present observations support the controversial results obtained by Goryczka et al. on a completely crystallized $Ti_{50}Ni_{25}Cu_{25}$ melt-spun ribbon, in which the existence of a 14 wt.% of B19′ phase in a B19 matrix was found by quantitative phase analysis performed with Rietveld refinement [21]. However, it has to be pointed out that in our case the monoclinic angle is notably lower (around 92°–93°) with respect to the monoclinic angle of the B19′ phase observed in $Ti_{50}Ni_{25}Cu_{25}$ (95.6°) [21] or in the $Ti_{50}Ni_{50-x}$-Cu_x system for $x \leqslant 10$ at.% Cu (96.8°) [15]. Therefore, this monoclinic structure could be the consequence of either a further decrease in the monoclinic angle of the same B19′ structure with increasing Cu content, as reported in [22] for compositions up to 10 at.% Cu, or to local deformations of the original orthorhombic structure.

5. Conclusions

An amorphous $Ti_{50}Ni_{25}Cu_{25}$ melt-spun ribbon has been partially crystallized by thermal treatments obtaining spherical particles, mainly in martensite, surrounded by large amorphous regions. TEM observations of these particles at RT show regions next to the crystalline–amorphous interfaces with retained austenite, as a result of the decrease of the martensitic transformation nearby these interfaces (i.e. a more stable austenite). Therefore, the effect of the amorphous interface is the same to that of a smaller grain size, which also decreases the transformation temperatures as a consequence of a higher surface/volume ratio, although the crystalline–amorphous interfaces show a higher effectiveness than the crystalline–crystalline grain boundaries in this sense. In addition, the use of new autoaccommodated structures nearby the interface with respect to the ones existing inside the particle has been observed in other particles. This further indicates the higher difficulties to undergo a normal martensitic transformation in the vicinity of the amorphous–crystalline interface.

Acknowledgements

This work was supported by the Training and Mobility Research program of the EEC under the project FMRX-CT98-0229 (DG12-BDN) entitled "Phase Transitions in Crystalline Solids". The authors also acknowledge Dr. A.V. Shelyakov for providing the ribbon studied in this work.

References

[1] Dutkiewicz J, Czeppe T, Morgiel J. Mat Sci Eng A 1999;273–275:703.
[2] Hu CT, Goryczka T, Vokoun D. Scripta Mater 2004;50:539.
[3] DeCristofaro N. Mater Res Bull 1998;23:50.
[4] Stoklosa Z, Rasek J, Kwapulinski P, Haneczok G, Badura G, Lelatko J. Mat Sci Eng C 2003;23:49.
[5] Kolomytsev V, Babanly M, Musienko R, Sezonenko A, Ochin P, Dezellus A, et al. J Phys IV 2001;11:457.
[6] Dalle F, Dezellus A, Elgoyhen C, Larnicol M, Masse M, Ochin P, et al. Final report of the E.U. INCO-Copernicus project IC15-CT96-0704;1999.
[7] Shi JD, Ma JL, Gao Y, Pu ZJ, Wu KH. In: Bormann R, Mazzone G, Shull RD, Averback RS, Ziolo RF, editors. Materials Research Society Symposium Proceedings, vol. 400. Warrendale: The Materials Research Society; 1996. p. 221.
[8] Schloßmacher P, Boucharat N, Rösner H, Wilde G, Shelyakov AV. J Phys IV 2003;112:731.
[9] Santamarta R, Pasko A, Pons J, Cesari E. Mater Trans (in press).
[10] Potapov PL, Shelyakov AV, Schryvers D. Scripta Mater 2001;44:1.
[11] Rösner H, Shelyakov AV, Glezer AM, Schloßmacher P. Mat Sci Eng A 2001;307:188.
[12] Satto C, Ledda A, Potapov P, Janssens JF, Schryvers D. Intermetallics 2001;9:395.
[13] Cesari E, Pons J, Santamarta R, Seguí C, Stróz D, Morawiec H. In: Morawiec H, Stróz D, editors. Proc XVIII Conference on Applied Crystallography. Singapore: World Scientific; 2001. p. 171.
[14] Santamarta R, Cesari E, Pons J, Goryczka T. Metall Mater Trans A 2004;35:761.
[15] Moberly WJ, Melton KN. In: Duerig TW, Melton NK, Stöckel D, Wayman CM, editors. Engineering Aspects of Shape Memory Alloys. London: Butterworth-Heinemann; 1990. p. 46.
[16] Saburi T. In: Otsuka K, Wayman CM, editors. Shape Memory Materials. Cambridge: Cambridge University Press; 1998. p. 49.
[17] Santamarta R, Schryvers D. Mater Trans 2003;44:1760.
[18] Santamarta R, Schryvers D. Intermetallics 2004;12:341.
[19] Watanabe Y, Saburi T, Nakagawa Y, Nenno S. J Japan Inst Metals 1990;54:861.
[20] Saburi T, Komatsu T, Nenno S, Watanabe Y. J Less-Common Met 1986;118:217.
[21] Goryczka T, Karolus M, Ochin P, Morawiec H. J Phys IV 2001;11:345.
[22] Nam TH, Saburi T, Nakata Y, Shimizu K. Mater Trans JIM 1990;31:1050.